

# Microscopic and macroscopic stress with gravitational and rotational forces

Wm. G. Hoover and Carol G. Hoover

Ruby Valley Research Institute, Highway Contract 60, Box 598, Ruby Valley, Nevada 89833, USA

James F. Lutsko

Center for Nonlinear Phenomena and Complex Systems, Université Libre de Bruxelles, CP 231, Blvd. du Triomphe, 1050 Brussels, Belgium

(Received 14 January 2009)

Many recent papers have questioned Irving and Kirkwood's atomistic expression for stress. In Irving and Kirkwood's approach both interatomic forces and atomic velocities contribute to stress. It is the velocity-dependent part that has been disputed. To help clarify this situation we investigate (i) a fluid in a gravitational field and (ii) a steadily rotating solid. For both problems we choose conditions where the two stress contributions, potential and kinetic, are significant. The analytic force-balance solutions of both these problems agree very well with a smooth-particle interpretation of the atomistic Irving-Kirkwood stress tensor.

DOI: XXXX

PACS number(s): 02.70.Ns, 45.10.-b, 46.15.-x, 47.11.Mn

## I. INTRODUCTION

In 2003 Zhou [1] published his lengthy and detailed paper "New Look at the Atomic Level Virial Stress" in the *Proceedings of the Royal Society of London*. He criticized the usual Irving-Kirkwood virial expression [2] for the pressure tensor  $P$  as a sum of potential and kinetic terms. The pressure tensor is the same thing as the comoving corotating momentum flux, and is also minus the stress tensor,  $\sigma \equiv -P$ . The detailed microscopic Irving-Kirkwood approach has been used for more than 50 years in the interpretation of atomistic molecular-dynamics simulations [3–6]. Averaged over a homogeneous periodic volume  $V$ , the Irving-Kirkwood expression for the pressure tensor gives

$$-\sigma V \equiv PV = P^{\Phi}V + P^KV = \sum_{i<j} (Fr)_{ij} + \sum_i (pp/m)_i.$$

Here  $F_{ij}$  is the force (for simplicity we assume a pairwise-additive potential) exerted on particle  $i$  by particle  $j$ , where the vector from  $j$  to  $i$  is  $r_{ij}$ . Particle  $i$ , at location  $r_i$  with mass  $m_i$  and momentum  $p_i$ , obeys Newton's equation of motion,

$$m_i \ddot{r}_i \equiv F_i^{\text{ext}} + \sum_{j \neq i} F_{ij}, \quad F_{ij} = -\nabla_i \phi(|r_{ij}|), \quad \Phi \equiv \sum_{i<j} \phi_{ij}.$$

Zhou [1] stated that only the tensor force sum,  $\Sigma(Fr)_{ij} \equiv \Sigma F_{ij} r_{ij}$ , contributes to the stress, while the tensor momentum sum,  $\Sigma(pp/m)_i \equiv \Sigma(p_i p_i / m_i)$ , does not.

This idea—including the forces but not the momenta—is not quite so outlandish as it seems. In solids, where the long-time average of the particle location is a sensible quantity, the virial theorem *can* be written in a similar tensor form omitting the momenta:

$$\langle PV \rangle = \sum_{i<j} \langle (FR)_{ij} \rangle, \quad R_i \equiv \langle r_i \rangle.$$

This form is derived in Sec. IIC of Ref. [4]. We use angular brackets here to indicate longtime averages. In situations including external forces the tensor force sum must also include either  $(F^{\text{ext}}r)_i$  or  $(F^{\text{ext}}R)_i$ .

Subramaniyan and Sun [7] tested Zhou's ideas [1] with molecular dynamics, heating a model atomistic solid subject to a variety of external boundary conditions on the particle coordinates. Their simulations showed that only the full Irving-Kirkwood pressure tensor, potential plus kinetic, was consistent with macroscopic thermodynamics. Liu and Qiu [8] recently provided a useful list of references supporting both sides of the question. In addition they suggested that the Zhou prescription is correct provided that external fields and rotation are not involved. Here we explore those latter two conditions separately and explicitly, showing that both (i) an external field (gravity) and (ii) a condensed-phase rotation can be analyzed properly with the Irving-Kirkwood pressure tensor, in a way compatible with macroscopic continuum mechanics. This suggests that the original Irving-Kirkwood approach is more generally useful than is the suggested modification of it by Zhou [1].

In order to compute continuous differentiable field variables (density, velocity, energy, stress, heat flux, etc.) from atomistic molecular-dynamics simulations, for comparison to corresponding fields generated by continuum mechanics solutions, we recommend the use of "smooth-particle" averages. These correspond to smearing individual particle properties over a spatial region of size  $h$ , the range of the smooth-particle weighting function, as described in a recent text [9], summarized in Sec. II, and applied in Sec. III.

Because the derivation of the pressure tensor is familiar and applies both at and away from equilibrium [4,5], we do not repeat that here. Instead, in Secs. III and IV, we describe and study two especially instructive problems involving gravitational and rotational forces. We reserve our conclusions and closing remarks for Sec. V.

## II. SMOOTH-PARTICLE AVERAGES OF ATOMISTIC PROPERTIES

Irving and Kirkwood [2] chose to localize *particle* properties at the particle locations using delta functions. Though this is convenient for formal analyses, and even natural for mass and momentum, a smoothed or smeared-out particle

86 contribution to potential energy and to fluxes often simplifies  
 87 comparisons with continuum mechanics. The smeared ap-  
 88 proach can provide field variables with two continuous spa-  
 89 tial derivatives, as we show below.  
 90 Because “action at a distance” makes the exact location of  
 91 momentum and energy fluxes ambiguous, we choose to  
 92 smear out particle contributions within a spatial region some-  
 93 what larger in extent than the spacing between particles. We  
 94 use a local weight function with a range  $h$ ,  $w(r, h)$ , to convert  
 95 particle properties to continuum field properties. Consider,  
 96 for example, the density  $\rho$  and the velocity  $v$  in a fluid or  
 97 solid composed of particles with individual masses and ve-  
 98 locities  $\{m_i, v_i\}$ . In the smooth-particle approach [9,10] field  
 99 variables, such as the density and velocity at the point  $r$ , are  
 100 defined as  $h$ -dependent (range-dependent) sums of nearby  
 101 particle contributions:

$$\rho(r) \equiv \sum_j m_j w(|r - r_j|),$$

$$\rho(r)v(r) \equiv \sum_j m_j v_j w(|r - r_j|).$$

102

103

104 The sums include all particles within a distance  $h$  of point  $r$ .  
 105 A good feature of this approach is that these definitions  
 106 of density and velocity satisfy the continuity equation  
 107  $\dot{\rho}/\rho \equiv -\nabla \cdot v$  exactly. Here, as usual, the dot indicates a co-  
 108 moving time derivative following the motion.

109 Lucy [10] was one of the inventors of the smooth-particle  
 110 approach. For convenience we use his form for the weighting  
 111 function in all of our smooth-particle sums,

$$w_{\text{Lucy}}^D(|r| < h) = C_D(1 - 6x^2 + 8x^3 - 3x^4), \quad x = |r|/h.$$

113 This form has two continuous derivatives everywhere. The  
 114 normalizing prefactor  $C_D$  depends on the dimensionality  $D$ ,

$$C_1 = (5/4h), \quad C_2 = (5/\pi h^2), \quad C_3 = (105/16\pi h^3).$$

116  $C$  is chosen so that the spatial integral of the weight function  
 117 is unity:

$$\int_0^h w^1(r)2dr = \int_0^h w^2(r)2\pi r dr = \int_0^h w^3(r)4\pi r^2 dr \equiv 1.$$

118

119 Lucy’s polynomial form [10] is the simplest normalized  
 120 weight function with a maximum value at the origin and two  
 121 continuous derivatives everywhere. In Sec. III, where we  
 122 consider the mechanical equilibrium of a two-dimensional  
 123 fluid in a one-dimensional gravitational field, we compute  
 124 average values of the pressure tensor using the one-  
 125 dimensional form of Lucy’s weight function [10].

### 126 III. GRAVITATIONAL EQUILIBRATION

127 Gravitational equilibration is a problem in which both the  
 128 potential and kinetic contributions to stress can play a role.  
 129 Where a constant gravitational acceleration acts downward  
 130 in  $y$ , the simple force-balance equation for mechanical equi-  
 131 librium is

$$dP/dy = (dP/d\rho)(d\rho/dy) = -\rho g. \quad 132$$

The stationary density profile  $\rho(y)$  can be found provided  
 that the dependence of pressure  $P$  on the density  $\rho$  is known.  
 As a simple example problem, chosen to highlight the kinetic  
 and potential contributions to the virial, we choose to study  
 the molecular dynamics of an atomistic system which closely  
 approximates the isothermal fluid equation of state

$$P(\rho, T) = (\rho^2/2) + \rho T, \quad T \equiv 1. \quad 139$$

This equation of state closely corresponds to the virial equa-  
 tion of state for two-dimensional particles of unit mass at  
 unit temperature interacting with a “cusp” potential chosen  
 to have a spatial integral of unity:

$$\phi_{\text{cusp}}(r < h) = (10/\pi h^2)(1 - x)^3, \quad x = |r|/h \quad 144$$

$$\rightarrow \int_0^h 2\pi r \phi_{\text{cusp}}(r) dr \equiv 1. \quad 145$$

$$\langle p_x^2/m \rangle = \langle p_y^2/m \rangle = kT \equiv 1. \quad 146$$

We use this cusp interaction for the interparticle forces  
 because the model closely corresponds to the simple and  
 useful thermodynamic equation of state given above. We  
 choose the range of the cusp pair potential  $h=3$ , so that the  
 deviation of the potential part of the pressure tensor from  
 that macroscopic equation of state is on the order of 1%.

For periodic two-dimensional systems the virial-theorem  
 expression for the potential part of the pressure tensor can be  
 expressed in terms of sums over all  $N(N-1)/2$  pairs of in-  
 teracting particles [4,5]. For a hydrostatic fluid, where  $P_{xx}^{\Phi}$   
 and  $P_{yy}^{\Phi}$  are each equal to the potential part  $P^{\Phi}$  of the hydro-  
 static pressure  $P$ , we have

$$P_{xx}^{\Phi} V = \sum (xF_x)_{i<j} \quad 159$$

$$= P_{yy}^{\Phi} V = \sum (yF_y)_{i<j} = (1/2) \sum (F \cdot r)_{i<j} = P^{\Phi} V. \quad 160$$

For a completely random distribution of particles in the vol-  
 ume  $V$ , the potential part of the pressure is then given by a  
 force integral. The integral can be related to the integral of  
 the pair potential using integration by parts. With our partic-  
 ular choice of pair potential  $\phi$ , with an integral of unity,  
 and particle mass, unity, the resulting hydrostatic pressure is  
 simply half the square of the density:

$$P^{\Phi} V = (1/2) \sum (F \cdot r)_{i<j} \quad 168$$

$$\approx -[N(N-1)/(4V)] \int_0^h 2\pi r^2 \phi' dr \quad 169$$

$$\equiv +[N(N-1)/(2V)] \int_0^h 2\pi r \phi dr \quad 170$$

$$\equiv N(N-1)/(2V) \approx N\rho/2 \rightarrow P^{\Phi} \approx (1/2)\rho^2. \quad 171$$

A snapshot from an isokinetic (constant-kinetic-  
 temperature) simulation appears in Fig. 1.

For convenience we have chosen a situation in which the  
 potential and kinetic parts of the pressure are equally

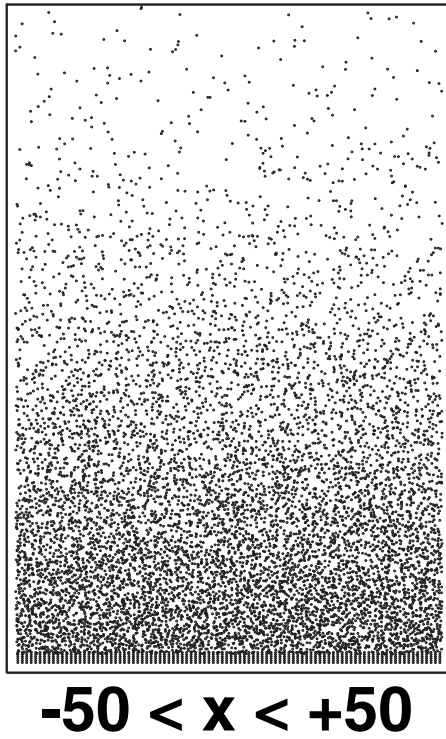


FIG. 1. Gravitational isothermal equilibrium at unit temperature for  $n_x n_y = 96 \times 96 = 9216$  moving particles above  $6 \times 96 = 576$  boundary particles fixed at the bottom of the system. The width of the system is  $n_x = 96$ . The height is unbounded. The field strength  $g = 4/n_y$  is chosen so that the maximum density matches that of the fixed particles at the bottom:  $\rho = N/V = 2$  at  $y = 0$ . This snapshot is typical of a long simulation used to calculate the smooth-particle pressure profiles shown in Fig. 2. In all of the figures dimensionless (or “reduced”) units are used. These follow from the definitions of unity for the particle mass, Boltzmann’s constant, and the length and energy scales in the interparticle forces derived from the cusp potential in Sec. II and the Hooke’s-law potential in Sec. IV.

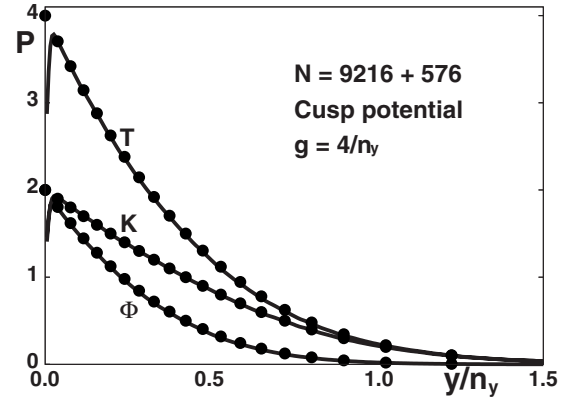


FIG. 2. Comparison of the observed and analytic pressure profiles for the gravitational problem shown in Fig. 1. From top to bottom the three curves are the total ( $T$  or Irving-Kirkwood), kinetic ( $K$ ), and potential ( $\Phi$  or Zhou) contributions to the pressure profile. These observed pressure contributions are calculated as smooth-particle averages. The points correspond to the analytic expressions from the isothermal equation of state  $P_T = P_\Phi + P_K = (\rho^2/2) + \rho$ .

$$F^{\text{rep}}(y < 0) \equiv -100y^3, \quad 192$$

which is applied to those few moving particles which occasionally penetrate the boundary at  $y = 0$ . 193

With periodic boundaries in  $x$  and a repulsive boundary at  $y = 0$ , a 9216-particle simulation gives the typical configuration we showed in Fig. 1. The corresponding kinetic and potential pressure profiles, averaged vertically with Lucy’s one-dimensional weight function [10], are compared to the analytic force-balance profile in Fig. 2. Evidently the agreement is quite good, and would be qualitatively in error were the kinetic contribution to the pressure tensor omitted. 194 195 196 197 198 199 200 201 202

#### IV. ROTATIONAL EQUILIBRATION 203

Next we consider the influence of the kinetic pressure on the mechanical equilibrium of a rotating *solid*. We can use molecular dynamics to determine the thermal (velocity-dependent) properties of an isolated *rotationless* crystal. For this study we have chosen a nearest-neighbor Hooke’s-law interaction, 204 205 206 207 208 209

$$\phi_{\text{Hooke}} = \frac{\kappa}{2} (|r| - d)^2, \quad 210$$

with the force constant  $\kappa$ , characteristic length  $d$ , and particle mass  $m$  all set equal to unity. To make contact with continuum mechanics we write the stress tensor in terms of the displacement vector  $u$  and elastic constants  $\lambda$  and  $\eta$ . 211 212 213 214

$$\sigma = \lambda \nabla \cdot u I + \eta [(\nabla u) + (\nabla u)^T], \quad 215$$

where  $I$  is the unit tensor, with  $I_{xx} = I_{yy} \equiv 1$  and  $I_{xy} = I_{yx} = 0$ . For the nearest-neighbor Hooke’s-law crystal the Lamé constants are known, 216 217 218

$$\lambda = \eta = \sqrt{3/16} \kappa, \quad 219$$

as is also the complete vibrational frequency distribution along with the bulk and surface entropies. See Chap. 4 of Ref. [5] for details. 220 221 222

176 important. At unit temperature ( $kT = 1$ ) and a density of  
177  $2$  ( $\rho = Nm/V = N/V = 2$ ), we have

$$178 \quad P^\Phi \simeq (N^2/2V^2) = \rho^2/2 = 2, \quad P^K = \rho kT = 2.$$

179 We choose the gravitational acceleration  $g$  so that the  
180 “weight” of a column of unit width and containing  $n_y$  par-  
181 ticles is equal to the maximum pressure, 4, at the maximum  
182 density,  $\rho(y = 0) = 2$ . In this case the mechanical equilibrium  
183 force-balance density and pressure profiles are

$$184 \quad (\rho + 1)(d\rho/dy) = -\rho g \rightarrow \rho - 2 + \ln(\rho/2) = -gy,$$

$$185 \quad P(y) = P^\Phi(y) + P^K(y) = g \int_y^\infty \rho(y) dy.$$

186 We test these analytic results against a molecular-  
187 dynamics simulation carried out *isothermally* [4–6] at a con-  
188 stant temperature of unity. At and below the bottom  $y = 0$  of  
189 the column, we place  $6n_x$  boundary particles in an area of  
190  $3n_x$  (corresponding to the maximum density, 2). See Fig. 1.  
191 We also include a short-ranged repulsive force,

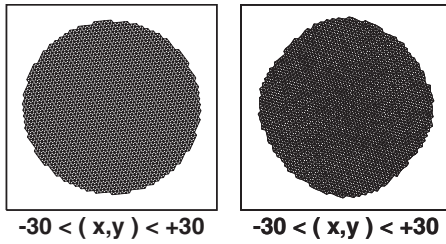


FIG. 3. Stationary rotation snapshots of two 2335-particle Hooke's-law crystals. In the rotationless stress-free case all 6828 nearest-neighbor distances are unity. In the steady rotational situations shown here, both with an angular frequency  $\omega=0.01$ , the tensile strain offsetting the centrifugal forces is maximized at the center of the rotating solid. The left view is a cold solid. The right view has a temperature  $kT=0.01$ .

223 The radial displacement in a rotating disk of radius  $R$ ,  
 224  $u(r)$ , as well as the corresponding stress tensor  $\sigma$ , is well-  
 225 known result of linear-elastic theory [11]. A derivation for  
 226 our two-dimensional situation is sketched in the Appendix.  
 227 The results are

$$228 \quad u(r) = (\omega^2 r / 18) [5R^2 - 2r^2],$$

$$229 \quad \sigma_{rr} = (\rho \omega^2 / 12) [5R^2 - 5r^2], \quad \sigma_{\theta\theta} = (\rho \omega^2 / 12) [5R^2 - 3r^2].$$

230 The stress components satisfy the radial force-balance equa-  
 231 tion for a plane-polar-coordinate volume element  $rdrd\theta$  ro-  
 232 tating at the angular frequency  $\omega$ :

$$233 \quad + \rho \ddot{r} = -\rho r \omega^2 = (d\sigma_{rr}/dr) + (\sigma_{rr} - \sigma_{\theta\theta})/r.$$

234 In the comoving and corotating frame, where stress is the  
 235 negative of the momentum flux, rotation provides a centrifug-  
 236 al force per unit mass varying as  $\omega^2$ .

237 To compare these results from linear elasticity to  
 238 molecular-dynamics simulations, consider the stationary rota-  
 239 tion of a Hooke's-law lattice. Figure 3 shows two nomi-  
 240 nally stationary states of a 2335-particle solid with an angu-  
 241 lar velocity of  $\omega=0.01$ . The cold crystal is shown at the left.  
 242 The kinetic temperature of the warm crystal shown on the  
 243 right is  $kT=0.01$ . The 2335-particle crystal is nearly circular.  
 244 It is the smallest with 36 particles equidistant from the origin  
 245 (at  $\sqrt{637} \approx 25.239$ ). Both these rotational problems were ini-  
 246 tialized by thermostating the radial momenta [4,5] while res-  
 247 caling the angular momenta to generate thermally equili-  
 248 brated, steadily rotating solid disks. During the first half of  
 249 each run two separate rescaling, or ‘‘Gaussian,’’ thermostats  
 250 were applied, so as to keep the radial temperature and the  
 251 angular velocity constant.

252 Figure 4 illustrates the approximately quadratic depen-  
 253 dence of the maximum tensile stress on the rate of rotation  
 254 for small angular velocities. For comparison with the simu-  
 255 lation results the linear-elastic stress at the center of a disk  
 256 with the same mass,  $Nm=2335$ , and a series of rotation rates  
 257  $\omega$  is also shown. The agreement is correct to four figures as  
 258  $\omega \rightarrow 0$ .

259 Let us next consider the stresses in a thermally excited  
 260 rotating crystal, computed according to the virial theorem  
 261 using the formulation of the atomistic stresses by Irving and

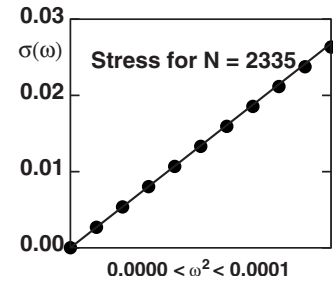


FIG. 4. Angular velocity dependence of the cold-crystal maximum tensile stress on rotation rate. The molecular-dynamics data, shown here as points, for nearly circular solids of the type shown in Fig. 3, agree with the linear-elastic result (shown as a straight line in the figure) for disks to four figures as the rotation rate goes to zero. The linear-elastic result is  $\sigma_{\max} V/N = (5N\sqrt{3}/4/12\pi)\omega^2$ .

Kirkwood [2]. The Hooke's-law nature of the particle inter-  
 262 actions guarantees that our model crystals will not melt. But  
 263 as temperature rises the deformation can become quite large,  
 264 so that linear-elastic theory no longer applies. Figure 5 is a  
 265 typical view of a rotating specimen at a rotation rate of  
 266  $\omega=0.01$  and a kinetic temperature (relative to rigid-body ro-  
 267 tation)  $kT=0.02$ .  
 268

The simplest route to the polar-coordinate stress tensor is,  
 269 first, to calculate the kinetic and potential parts of each partic-  
 270 le's pressure tensor in Cartesian coordinates:  
 271

$$(P_{xx}^K V)_i = (p_x^2/m)_i, \quad (P_{xy}^K V)_i = (p_x p_y/m)_i, \quad (P_{yy}^K V)_i = (p_y^2/m)_i, \quad 272$$

$$(P_{xx}^\Phi V)_i = \frac{1}{2} \sum_j (xxF/r)_{ij}, \quad (P_{xy}^\Phi V)_i = \frac{1}{2} \sum_j (xyF/r)_{ij}, \quad 273$$

$$(P_{yy}^\Phi V)_i = \frac{1}{2} \sum_j (yyF/r)_{ij}. \quad 274$$

In keeping with the Irving-Kirkwood picture, the potential  
 275 contributions to the pressure tensor are divided evenly be-  
 276 tween pairs  $\{i,j\}$  of interacting particles. The polar-  
 277 coordinate representation for each particle's pressure tensor  
 278 follows from the Cartesian representation by a simple rota-  
 279 tion, which can be written as a pair of matrix multiplications:  
 280

$$(PV)_{\text{polar}} = R \cdot (PV)_{\text{Cartesian}} \cdot R^t, \quad 281$$

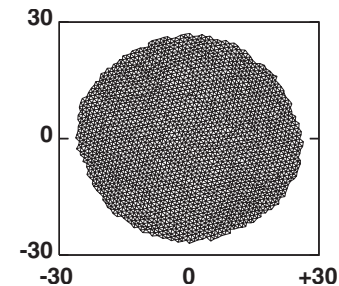


FIG. 5. View of a rotating 2335-particle Hooke's-law crystal at an angular velocity of 0.01 and a temperature  $kT=0.02$ .

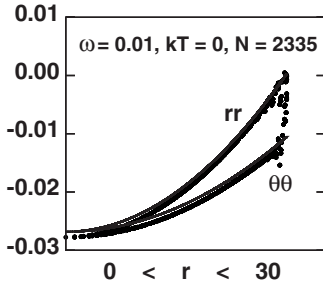


FIG. 6.  $PV$  in the rotating cold crystal in Fig. 3 with  $\omega=0.01$ . The theoretical radial and circumferential components are shown as lines based on the expressions derived in the Appendix.

$$R_i = \begin{bmatrix} +\cos(\theta_i) & +\sin(\theta_i) \\ -\sin(\theta_i) & +\cos(\theta_i) \end{bmatrix}, \quad \theta_i = \arctan(y/x)_i.$$

282

283 Figure 5 illustrates a thermally excited rotating Hooke's-  
284 law crystal. For the figure we have chosen the temperature so  
285 that the thermal stresses make a significant contribution to  
286 the pressure tensor. The radial stress vanishes at the disk  
287 boundary, while the circumferential “hoop” stress remains  
288 tensile there in conformity to the predictions of linear elas-  
289 ticity.

290 The stresses in two rotating crystals, one cold and one hot,  
291 are compared with the theoretical results from elastic theory  
292 in Figs. 6 and 7. The agreement is nearly perfect, and would  
293 be spoiled if the kinetic contributions were not included. In  
294 particular, omitting the kinetic contribution to the radial  
295 stress would be quite inconsistent with the vanishing of that  
296 stress component at the boundary of the disk.

297

## V. CONCLUSION

298 Both the gravitational and the rotational problems show  
299 excellent correspondence between conventional continuum  
300 mechanics and atomistic mechanics *provided that both the*  
301 *kinetic and potential parts of the pressure tensor are in-*  
302 *cluded* in the analysis. Although for stationary solids the  
303 solely potential form for the virial theorem is correct, the  
304 number and type of problems which can be studied numeri-  
305 cally are greatly enhanced by including the ideas of Irving  
306 and Kirkwood [2] coupled with the smooth-particle averag-  
307 ing introduced by Lucy and Monaghan in 1977. For well-  
308 defined local properties, both at and especially away from  
309 equilibrium, it is essential that these properties be measured  
310 in a coordinate frame that moves with the material. It is no  
311 accident that the fundamental equations of continuum me-  
312 chanics take their simplest form in the comoving frame. In  
313 particular, the pressure (or stress) and temperature tensors, as  
314 well as the heat flux, only make sense in this frame. Stress  
315 and pressure cannot depend upon the chosen coordinate sys-  
316 tem. Hence we must choose the “comoving” “corotating”  
317 “Lagrangian” frame. In that frame the pressure tensor is sim-

342

343

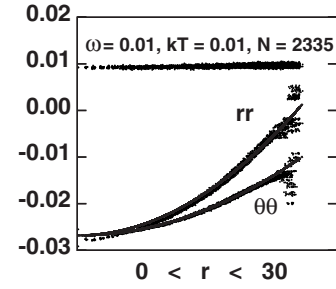


FIG. 7. Time-averaged stresses in the warm rotating thermally excited crystal in Fig. 3 with  $\omega=0.01$  and  $kT=0.01$ . The thermal contributions to  $(PV)_{rr}$  and  $(PV)_{\theta\theta}$  are the points at the top. The theoretical expressions for the stress (based on the cold-crystal elastic constant) shown as lines in the figure agree well with the points representing results from molecular dynamics. The molecular-dynamics results include both the potential and kinetic contributions to the comoving corotating stresses.

ply the momentum flux, and has both potential and kinetic 318  
contributions, as shown clearly in the two problems solved 319  
here. 320

## APPENDIX

321

The stationary rotation, at angular velocity  $\omega$ , of an elastic 322  
disk of radius  $R$  with equal Lamé constants  $\lambda = \eta = \sqrt{3}/16$  323  
obeys the force-balance equation in the comoving frame, 324

$$0 = +\rho\omega^2 r + (\partial\sigma_{rr}/\partial r) + (\sigma_{rr} - \sigma_{\theta\theta})/r. \quad 325$$

This macroscopic problem corresponds to a microscopic 326  
model composed of unit-mass particles linked by nearest- 327  
neighbor Hooke's-law springs. Both the spring constant and 328  
the rest length of the springs are taken equal to unity. The 329  
displacement responsible for the radial strain  $\epsilon_{rr} = (du_r/dr)$  330  
causes a corresponding strain in the circumferential direc- 331  
tion,  $\epsilon_{\theta\theta} = (u/r)$ . The stresses 332

$$\sigma_{rr} = \eta[3(du/dr) + (u/r)], \quad \sigma_{\theta\theta} = \eta[(du/dr) + 3(u/r)] \quad 333$$

convert the force balance to an ordinary differential equation, 334

$$r^2(d^2u/dr^2) + r(du/dr) - u = -\omega^2 r^3 \rho / (3\eta), \quad 335$$

with a unique solution such that the radial stress vanishes at 336  
 $R$ : 337

$$u(r) = (\rho\omega^2 r / 48\eta)[5R^2 - 2r^2] = (\omega^2 r / 18)[5R^2 - 2r^2]. \quad 338$$

This solution can be used to generate the maximum tensile 339  
stress in the disk as well as the stress and strain profiles, 340

$$\sigma_{rr} = (\rho\omega^2 / 12)[5R^2 - 5r^2], \quad \sigma_{\theta\theta} = (\rho\omega^2 / 12)[5R^2 - 3r^2]. \quad 341$$

**AQ: 344** [1] M. Zhou, Proc. R. Soc. London, Ser. A **459A**, 2347 (2003).  
**#1 345** [2] J. H. Irving and J. G. Kirkwood, J. Chem. Phys. **18**, 817  
**346** (1950).  
**347** [3] B. J. Alder and T. E. Wainwright, J. Chem. Phys. **31**, 459  
**348** (1959).  
**349** [4] Wm. G. Hoover, *Molecular Dynamics*, Lecture Notes in Phys-  
**350** ics Vol. 258 (Springer, Berlin, 1986), available at the home-  
**351** page <http://williamhoover.info/MD.pdf>  
**352** [5] Wm. G. Hoover, *Computational Statistical Mechanics*  
**353** (Elsevier, Amsterdam, 1991), available at the homepage [http://](http://williamhoover.info/book.pdf)  
**354** [williamhoover.info/book.pdf](http://williamhoover.info/book.pdf)  
**355** [6] D. J. Evans and G. P. Morriss, *Statistical Mechanics of Non-*  
*equilibrium Liquids* (Academic, London, 1990), available at **356**  
the authors' websites. **357**  
[7] A. K. Subramaniyan and C. T. Sun, Int. J. Solids Struct. **45**, **358**  
4340 (2008). **359**  
[8] B. Liu and X. Qiu, e-print arXiv:0810.0803. **360 AQ:**  
[9] Wm. G. Hoover, *Smooth Particle Applied Mechanics—The #2*  
*State of the Art* (World Scientific, Singapore, 2006), available **361**  
from the publisher at the publisher's site, [http://](http://www.worldscibooks.com/mathematics/6218.html) **362**  
[www.worldscibooks.com/mathematics/6218.html](http://www.worldscibooks.com/mathematics/6218.html) **363**  
[10] L. B. Lucy, Astron. J. **82**, 1013 (1977). **365**  
[11] T. B. Bahder, e-print arXiv:physics/0211004. **366**

**AUTHOR QUERIES —**

- #1 Please verify content of Ref. 1.
- #2 AU: Please update Refs. 8 and 11 if possible.